International Journal of Pioneering Technology and Engineering

Research Article

Power and Thermal Analysis of A Pcm-Cooled Photovoltaic Thermal System With A 1-D Mathematical Model for Different Environmental and Boundary Conditions: A Case Study

Erkan Ökten [a*] Levent Kırcı[a] Özgür Kılıçlı[b]

[a] Yenimahalle Mehmet Rüştü Uzel Vocational and Technical Anatolian High School, Ankara, Türkiye
[b] Çankaya Balgat Aliye Yahşi Vocational and Technical Anatolian High School, Ankara, Türkiye

Article Info

Article history
Received: 03/11/2023
Revised: 01/12/2023
Accepted: 13/12/2023

Keywords:
Mathematical Model,
Phase Change Material,
Photovoltaic Panel

ABSTRACT

Reducing the PV panel temperature significantly increases the PV panel efficiency. The most important parameters affecting the temperature of the PV panel are; environmental temperature, wind speed, sunbathing time, and irradiation. Although there are many methods for PV panel cooling, one of the most common methods is to cool the panel by placing PCM material on the PV panel's bottom surface. In this study, PV/PCM integration under different boundary conditions was investigated with a 1-D mathematical model. In the study, environmental conditions were determined using real meteorological data, and the results were shared for four seasons. The mathematical model was performed for the conventional PV model, the PV/PCM integrated model, and the integrated PV/PCM which the base is kept at a constant temperature. As a constant temperature value, 10, 15, and 20 ^{o}C were chosen. The results were analyzed in terms of PV temperature, PCM melting rate, electricity production, energy absorbed by PCM, and thermal and electrical efficiency. If the annual performances are examined, the maximum electricity production is 263000 kW for the case where the PV/PCM base is kept constant at 10 degrees, and this value is 1200 kW higher than the traditional PV panel. The maximum absorbed energy by PCM was obtained as 26990 kW for the PV/PCM integration.

1. Introduction

PV (Photovoltaic cell) panels are economical systems that generate electricity from solar energy [1]. Although PV panels have many advantages, they are highly affected by temperature and decrease in performance. Therefore, it is very important to reduce the PV panel operating temperature [2]. Two different methods are used to use the PV panel temperature. These methods are called active and passive cooling. An example of passive cooling is placing fins on the PV panel base or cooling the panel by natural convection of air. An example of active cooling is the cooling of the panel by passing water or air through the channel added to the bottom of the channel by forced convection [3-5].

One of the most effective passive methods of PV panel cooling is the integration of PCM (Phase Change Material). With this method, a container with a PCM is placed at the bottom of the PV panel. So, a significant amount of thermal energy is absorbed during solid liquid phase transition at constant temperature by PCM [6, 7]. There are many experimental and numerical studies examining PV-PCM performance in the literature. The studies can be grouped into two categories. The first of these is the examination of the PV/PCM panel performance in different environmental conditions, and the second is the effect of the changes in the components used in the system on the PV/PCM panel performance[8].

If the first group of studies is examined, Armstrong and Hurley [9] investigated the variation of PV panel temperature under forced and natural convection conditions for different wind speed and wind direction values. Smith et al. [10] conducted a study on the selection of the most accurate PCM material depending on the environmental conditions in different parts of the world. PV-PV/PCM panel performance was compared depending on the amount of radiation changing during the day by Stropnik et al [11]. Khanna et al. İnvestigated the effect of wind direction, wind velocity ,and ambient temperature on PV/PCM panels efficiency[12]. Savvakis and Tsoutsos investigated the performance of PV/PCM panel under real environmental conditions for one year under Mediterranean climatic conditions [13].

The second group of studies includes the effect of the innovations made in the components of the PV-PCM system on the system efficiency. Emam and Ahmed [6] integrated different types of PCM heat sinks such as single cavity, three-parallel cavity, five-parallel cavity, and three-series cavity to PV panel. In the study, PV panel performance was also investigated by adding different types of PCM materials to each cavity. Abdulmunem et al. [1] investigated the PCM melting characteristics and the temperatures of the components that make up the system for different tilt angles. Ahmad et al.[14] used 6 different configurations for panel cooling and compared with each other. These configurations are; PV, PV/water cooler, PV/PCM, PV/PCM/water cooler, PV/PCM/composite,

***Corresponding author:** Erkan Ökten
*E-mail address: sevgilierkan@gmail.com
https://doi.org/10.56158/jpte.2023.57.2.02

PV/PCM/composite/water cooler. Duan [15] designed the PCM media as porous to reduce the natural convection effects due to the melting of the PCM material. In addition to the above-mentioned approaches in the literature, there are studies that reduce the PV panel temperature by placing fins [16-18] in the PCM media or using a PCM/nanoparticles combination [19, 20].

When the studies in the literature were examined, PV/PCM system analysis has been made using numerical and experimental methods, the melting process and panel temperatures of PCM was examined or some improvements were made to the system. However, there are limited studies that mathematically examine PV/PCM performance under real operating conditions. As it is known, although mathematical models were performed under certain assumptions, they provide significant savings in terms of both computation time and cost. Therefore, in this study, the melting process of PCM and PV panel temperature were investigated under real ambient conditions by creating a 1-D mathematical model. The examinations were carried out for 5 different cases. First case; conventional PV panel, 2nd case PV panel PCM integration, 3rd case PCM container's bottom surface 10 ^{o}C boundary condition, 4th case PCM container's bottom surface 15 ^{o}C boundary condition, 5th case PCM container's bottom surface 20^{o}C boundary condition. Environmental conditions were determined using the meteorological data of Antalya province in Turkey. The results were analyzed in terms of PV panel temperature, PV panel efficiency, thermal efficiency, electricity production, thermal energy stored in PCM and PCM melting amounts. By carrying out these examinations, the advantages and disadvantages of the PV-PCM container, which has not been examined before in the literature, being immersed in the water channel at a constant bottom temperature, were determined.

2. System Description

Increasing the temperature of the PV cell significantly reduces the panel efficiency. Due to its energy storage capacity in solid-state and during phase change, PCM can take significant heat from the PV cells and reduce the PV cell temperature when placed under the PV panel. Therefore, in this study, a PCM container with different boundary conditions was placed under the PV panel to reduce the PV panel temperature. Within the scope of the study, 5 different cases were investigated. In case 1, the conventional PV panel was examined. In case 2, a PCM container was placed under the PV panel. The bottom of the container was considered to be open to the atmosphere. In Case 3, Case 4, and Case 5; similarly in Case 2, the PCM container was placed under the PV panel, but the container base temperature was considered to be constant. The constant temperature was taken as 10 ^{o}C for Case 3, 15 ^{o}C for Case 4, and 20 ^{o}C for Case 5. Indeed, it is unlikely that the bottom of the PCM container will be at a constant temperature. However, in this study, the bottom of the PCM container was considered to be in contact with a water source. Since the water source temperature is unknown, the results were examined for three different temperatures.

A polycrystalline PV panel (12.5x12.5 cm) was used in the study and the panel consists of a glass cover, an EVA layer, an aluminum layer, PCM, and PCM container layers. The thickness and thermal properties of each layer were shown in Table 1. It was assumed that the PV panel side surfaces were completely insulated. In order to determine the PV panel length, the environmental conditions in which the maximum melting (in Case 2 and summer conditions) was taken into account, and it was determined as 0.0276 m.

Table 1. Thermal properties thicknesses of PV panel components

	Thickness (m)	Conductivity (W/mK)	Emissivity	Temperature coefficient (1/K)	Reference efficiency, η_{ref}	References
Glass Cover	0.003	0.8	0.9	-	-	[21]
PV Layer	0.0002	148		0.0045	0.2	[6]
EVA	1.27 x 10^{-6}	0.37	-	-	-	[21]
Aluminium	0.004	211	0.095	-	-	[21]

2.1. Mathematical Modeling

In this study, 3 different mathematical models were created for the 5 cases examined. For Case 1, only the PV panel was chosen as the control volume and a solution was obtained using thermal resistance networks (Fig. 1). In all other cases, firstly, the PV panel was chosen as the control volume and modeled with thermal resistance networks, then the PCM container was chosen as the control volume and the analytical solution was obtained (Fig 2.,3.). Since the thermal resistance network model was used for the PV panel in all 5 cases, the common thermal resistors in each case were examined below.

Considering the PV panel energy balance, some of the solar radiation sourced energy coming to the PV panel surface is converted into electrical energy, and some are lost to the atmosphere from the lower and upper surface of the PV panel. The heat lost from the panel surfaces are generated by convection and radiation. Losses by convection depend on ambient temperature (T_a), and losses by radiation depend on surrounding temperature (T_{surr}). In order to facilitate the calculations, the two temperatures are taken as equal in this study [22].

Based on this assumption, the combined heat transfer coefficient (h_{comb})was calculated as follows.

$$h_{comb} = h_{conv} + h_{rad} \quad (1)$$

In Eq.1. $h_{conv}$and h_{rad}represent convection and radiation heat transfer coefficient respectively and were calculated as follows [23].

$$h_{conv} = 2.8 + 3V_{wind} \quad (2)$$

$$h_{rad} = A_{pv}\sigma\varepsilon(T_s^2 + T_{surr}^2)(T_s + T_{surr}) \quad (3)$$

In Eq. 2, V_{wind} is wind velocity. In Eq. 3, $A_{pv}$is PV panel area and taken as 1 m2, σ is the Stefan Boltzmann constant, ε is the emissivity and T_s (upper or lower surfaces) is the surface temperature.

The combined thermal resistance formed by the heat loses from the surfaces as follows.

$$R_{comb} = \frac{1}{h_{comb}A_{PV}} \quad (4)$$

The thermal resistances formed by the glass, EVA(ethylene-vinyl acetate) ,and aluminum layer are as follows.

$$R_{glass} = \frac{L_{glass}}{k_{glass}A_{PV}} \quad (5)$$

$$R_{EVA} = \frac{L_{EVA}}{k_{EVA}A_{PV}} \quad (6)$$

$$R_{Al} = \frac{L_{Al}}{k_{AL}A_{PV}} \quad (7)$$

In Eq. 5, $L_{glass}$is thicknesses of glass layer and k_{glass} is thermal conductivity of glass layer. In Eq. 6, $L_{EVA}$is thicknesses of EVA layer and k_{EVA} is thermal conductivity of EVA layer. In Eq. 7, $L_{Al}$is thicknesses of aliminium layer and k_{AL} is thermal conductivity of aliminium layer.

Firstly, the mathematical model created for Case 1 was examined below.

Case 1;

In Case 1, the conventional PV panel was examined. The

physical, heat transfer, and thermal resistance network model for Case 1 is shown in Figure 1. In the conventional PV panel, while some of the solar radiation energy coming to the PV cell is converted into electrical energy, some of it's lost to the environment on the upper and lower surface of the PV panel. Therefore, if the PV panel is selected as the control volume, the heat loss from the top and bottom surface of the PV panel is equal to the total heat loss.

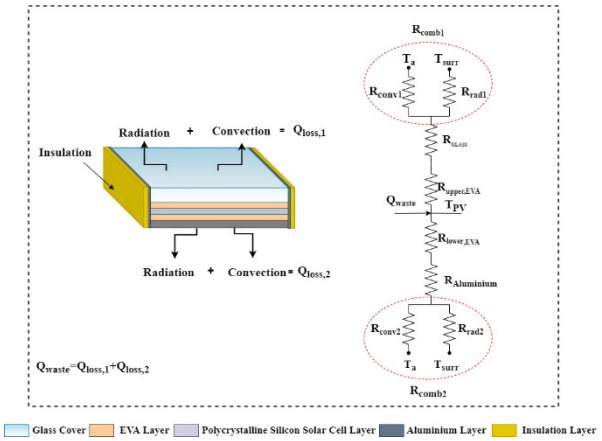

Fig. 1. Physical, heat transfer and the thermal resistance network model for Case 1.

The heat loss from the PV panel upper surface was defined as in Eq. 8.

$$\dot{Q}_{loss,1} = \left(\frac{T_{s,up}-T_{surr}}{R_{comb,up}}\right) = \left(\frac{T_{pv}-T_{surr}}{R_{EVA,up}+R_{glass}+R_{comb,up}}\right) \quad (8)$$

In Eq.8, $T_{s,up}$is upper surface temperature of PV panel and$R_{comb,up}$,$R_{EVA,up}$, R_{glass} are upper surface combined thermal resistance, upper EVA thermal resistance and glass thermal resistance respectively. The heat loss from the lower surface of the PV panel will be as in Eq. 9.

$$\dot{Q}_{loss,2} = \left(\frac{T_{s,lower}-T_{surr}}{R_{comb,lower}}\right) = \left(\frac{T_{pv}-T_{surr}}{R_{EVA,lower}+R_{al}+R_{comb,lower}}\right) \quad (9)$$

In Eq.9, $T_{s,lower}$is lower surface temperature of PV panel and$R_{comb,lower}$,$R_{EVA,down}$, R_{glass} are lower surface combined thermal resistance, lower EVA thermal resistance and aliminium thermal resistance respectively. Finally, it is defined that the total heat loss ($\dot{Q}_{waste}$) is equal to the sum of the heat loss from the lower ($\dot{Q}_{loss,1}$) and upper ($\dot{Q}_{loss,2}$) surface of the PV panel.

$$\dot{Q}_{waste} = \dot{Q}_{loss,1} + \dot{Q}_{loss,2} \quad (10)$$

For the solution of Case 1, only the thermal resistance networks model was used. For the solution of Case 2, the thermal resistance network and analytical model were used together.

Case 2;

The physical, heat transfer, and thermal resistance model of the PV-PCM integration examined in Case 2 is shown in Fig. 2. The PV/PCM integration was divided into two parts. Firstly, the PV panel was chosen as the control volume and solved with thermal resistance networks, and secondly, the PCM container was chosen as the control volume and the analytical solution was obtained. . In Case 2, while some of the solar radiation energy coming to the PV cell is converted into electrical energy, some of it's lost to the environment on the upper of the PV panel, and some of it passes under the panel to the PCM container. The thermal energy transferred to the PCM ($\dot{Q}_{PCM}$) container is equal to the sum of the energy stored by the PCM phase change and the heat loss from the bottom of the container to the environment.

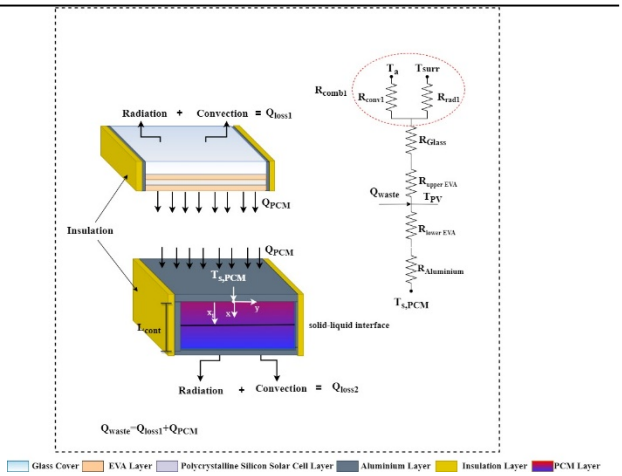

Fig. 2. Physical, heat transfer and the thermal resistance network model for Case 2.

The energy balances used in PV panel analysis modeled with thermal resistance networks are as follows.

Eq. 11 shows the heat loss from the panel upper surface to the atmosphere.

$$\dot{Q}_{loss,1} = \left(\frac{T_{s,up}-T_{surr}}{R_{comb,up}}\right) = \left(\frac{T_{pv}-T_{surr}}{R_{EVA,up}+R_{glass}+R_{comb,up}}\right) \quad (11)$$

Eq 12. shows the heat transferred from the PV panel to the surface of the PCM container. In Eq., $T_{s,PCM}$is PCM container upper surface temperature.

$$\dot{Q}_{PCM} = \left(\frac{T_{pv}-T_{s,PCM}}{R_{EVA,lower}}\right) \quad (12)$$

The heat loss in the PV panel is defined as follows.

$$\dot{Q}_{waste} = \dot{Q}_{loss,1} + \dot{Q}_{PCM} \quad (13)$$

Following the PV panel analysis, the PCM container was analytically modeled. In this study, since the PCM container was placed horizontally, the convection effects due to the melting of the PCM material were neglected. Therefore, the 1-D time-dependent heat conduction equation will be as follows.

$$\frac{\partial^2 T}{\partial x^2} = \frac{1}{\alpha}\frac{\partial T}{\partial t} \quad (14)$$

The expression αseen in the Eq. 14 is thermal diffusivity and is defined as $\frac{k}{\rho c_p}$. In phase change problems, when latent heat is more dominant than sensible heat, in other words, when Ste<0.1, The time dependent term seen in Eq. 14 can be neglected [24]. Therefore, for the liquid phase Eq. 14 take the following form.

$$\frac{\partial^2 T_l}{\partial x^2} = 0 \quad (15)$$

The boundary conditions shown below are used to solve Eq. 15.

$$x = 0, \; -k_l\frac{\partial T_l}{\partial x} = \frac{\dot{Q}_{PCM}}{A} \quad (15a)$$

$$x = x_i, T_l = T_m \quad (15b)$$

As seen in Eq. 15a and 15b, the heat flux boundary condition from the top surface of the PCM container and the constant melting temperature (T_m) boundary condition at the solid-liquid interface are used for the solution. The solid phase heat conduction equation is as follows.

$$\frac{\partial^2 T_s}{\partial x^2} = 0 \quad (16)$$

The boundary conditions shown below were used to solve Eq. 16.

$$x = x_i, T_s = T_m \quad (16a)$$

$$x = L_{cont}, \; \frac{\partial T_s}{\partial x} = -\frac{h_{comb}}{k_s}(T_p - T_a) \quad (16b)$$

As seen in Eq. 16 a and 16 b, the boundary condition of constant melting temperature (T_m) was used at the liquid-solid interface, and the boundary condition of heat loss from the temperature T_p to the environment at the bottom of the container

was used. Using the equation (Eq.15, Eq.16) and boundary conditions seen above for the liquid and solid phases, the solutions were obtained as follows.

$$T_l(x) = \frac{\dot{Q}_{PCM}}{A_{pv}k_l}(x_i - x) + T_m \quad (17)$$

$$T_s(x) = \frac{h_{comb}}{k_s}(T_p - T_a)(x_i - x) + T_m \quad (18)$$

With the help of Eq. 18, T_p temperature was found as follows. The bottom surface thermal resistance of the PCM container was neglected in the calculations.

$$T_p = \left(\frac{\left(-h_{comb}.\frac{(x_i - L_{cont})T_a}{k_s}\right) + T_m}{1 - \left(h_{comb}\frac{x_i - L_{cont}}{k_s}\right)}\right) \quad (19)$$

The boundary condition for examining the time dependent change of the solid-liquid interface is as follows [24].

$$k_s \frac{\partial T_s(x_i,t)}{\partial x} - k_l \frac{\partial T_l(x_i,t)}{\partial x} = \rho_l L \frac{dx_i}{dt} \quad (20)$$

The following initial condition was used to solve Eq.20.

$$x_i(0) = 0 \quad (21)$$

If Eq. 17 and 18 are written in Eq. 20, the time dependent x_i function is obtained as follows.

$$x_i(t) = \left(\left(\left(\left(-h_{comb} \cdot (T_p - T_a)\right) + (\dot{Q}_{PCM}/A_{pv})\right)\right) \cdot \frac{t}{\rho_l \cdot L}\right) \quad (22)$$

In Case 3, 4, and 5, unlike Case 2, the container base temperature was kept constant. Solution details are shown below.

Case 3, Case 4, Case5;

In Cases 3 ($T_p = 10^oC$), 4 ($T_p = 15^oC$) and 5 ($T_p = 20^oC$) unlike Case 2, the bottom of the PCM container was kept at a constant temperature (Fig. 3). The PV panel solution is the same as for Case 2 and for Case 3, 4, and 5. Therefore, Eq. 11, 12, and 13 were also used in Case 3, 4, and 5. An analytical model was created to calculate the temperature distribution and phase transition region of the PCM in the container. The model used for the liquid phase is the same as Case 2. Therefore, the liquid phase solution is as seen in Eq. 17. For the solid phase, a constant temperature (T_p) boundary condition was applied to the bottom surface of the PCM filled container. The heat conduction equation and boundary conditions are as follows.

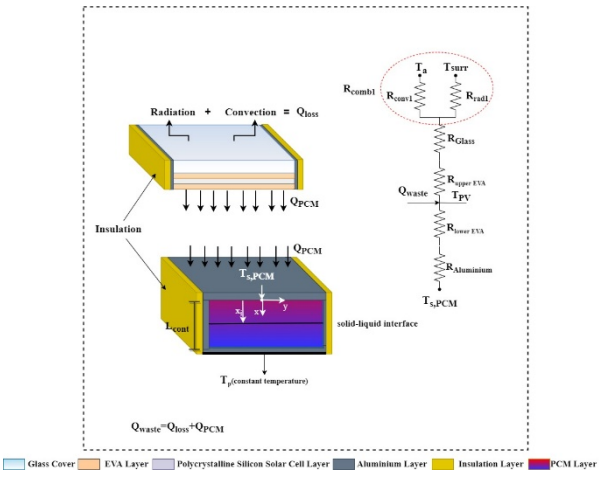

Fig. 3. Physical, heat transfer and the thermal resistance network model for Case 3,4 and 5.

$$\frac{\partial^2 T_s}{\partial x^2} = 0 \quad (23)$$

$$x = x_i, T_s = T_m \quad (23a)$$

$$x = L_{cont}, T_s = T_p \quad (23b)$$

If Eq. 23 is solved using boundary conditions, the solution for the solid phase is as follows.

$$T_s(x) = \frac{(T_m - T_p)}{(x_i - L_{cont})}(x - x_i) + T_m \quad (24)$$

The temperature at the base of the container is T_s=T_p.

Eq.25 shows the variation of the solid-liquid interface of the PCM material time-dependent. Eq. 25 was obtained by substituting Eq. 24 and 17 in Eq. 21 using the boundary condition seen in Eq. 22.

$$t = \frac{\rho_l L}{\dot{Q}_{PCM}} - \frac{\rho_l L k_s (T_m - T_p)}{\dot{Q}_{PCM}^2} ln \frac{k_s(T_m - T_p) + \dot{Q}_{PCM}(x_i - L_{cont})}{k_s(T_m - T_p) - \dot{Q}_{PCM}L_{cont}} \quad (25)$$

The system outputs reached through the solution process detailed above are seen below. Eq.26 shows the efficiency of the PV panel [6].

$$n_{pv} = n_{ref}\left(1 - \beta_{ref}(T_{pv} - T_{ref})\right) \quad (26)$$

n_{ref} and β_{ref} are the reference solar cell efficiency and the solar cell temperature coefficient at a reference temperature (T_{ref}) seen in Eq. 26. T_{ref} value was taken as 25 ^oC and $\beta_{ref}$and n_{ref}values were given in Table 1. The net thermal power input ($\dot{Q}_{netPV}$) to the PV panel from solar radiation is shown in Eq. 27 [21].

$$\dot{Q}_{netPV} = G n_{op} A_{pv} \quad (27)$$

seen in Eq. 27, G is irradiation, $n_{op}$is optical efficiency and was taken as 0.85. In Eq.28, the expression of net electrical power produced in the PV panel is seen [21].

$$\dot{W}_{elPV} = \dot{Q}_{netPV} n_{pv} n_{inv} \quad (28)$$

n_{inv} seen in Eq. 28 is the inverter efficiency and it was taken as 0.9. Eq.28 shows the expression the waste heat from the panel to the environment [21].

$$\dot{Q}_{waste} = \dot{Q}_{netPV}(1 - n_{pv}) \quad (29)$$

Eq. 30 and 31 show the energy absorbed by the PCM and thermal efficiency respectively.

$$\dot{Q}_{abs} = m_l(T_m - T_a) + m_l L \quad (30)$$

$$n_{th} = \frac{\dot{Q}_{abs}}{G A_{pv} t} \quad (31)$$

The m_l seen in Eq. 30 represents the mass of the liquid phase in the PCM container.

2.2. PCM Selection and Thermal Properties

One of the most important parameters in PCM selection is the melting temperature. In the study was carried out by Me et al, they found that the PV panel is cooled more when the melting temperature of the PCM is higher than the ambient temperature [8]. Therefore, RT28HC material with a melting temperature of 28 ^{o}C was chosen in this study (In this study, the maximum ambient temperature is 27 ^{o}C). PCM material thermal properties were given in Table 2.

Table 2. Thermal properties of the PCM [11].

Thermal Properties	Value
Melting temperature (^{o}C)	28
Latent heat of fusion (kJ/kg)	245
Thermal conductivity (W/m K)	0.2
Density (solid) (kg/m^3)	880
Density (liquid) (kg/m^3)	770
Specific heat capacity (kJ/kg K)	2

2.3.Solution Procedure

As seen in Fig. 4, two different models were created for Case 1 and for Case 2,3,4 and 5. The created model was analyzed using the EES program. Input parameters shown in Fig. 4 were defined in both model solutions. For Case 1, system outputs were obtained using only PV panel equations (Eq.8,9,10). For Cases 2,3,4 and 5, the $T_{s,PCM,Guess}$value was estimated primarily. Then, the $\dot{Q}_{PCM}$value was calculated using the PV panel equations (Eq. 11,12,13). A $T_{s,PCM,Calculated}$ was calculated by taking the $\dot{Q}_{PCM}$

value as an input to the equations created for the Analytical solution (Eq. 17,18,19,22 for Case 2 and Eq. 17, 24,25 for Case 3,4,5). Finally, $T_{s,PCM,Guess}$ and $T_{s,PCM,Calculated}$ were compared and if the difference was less than 10-3, the system outputs were found. If not, the new $T_{s,PCM,Guess}$ was taken equal to $T_{s,PCM,Calculated}$ and the process was repeated.

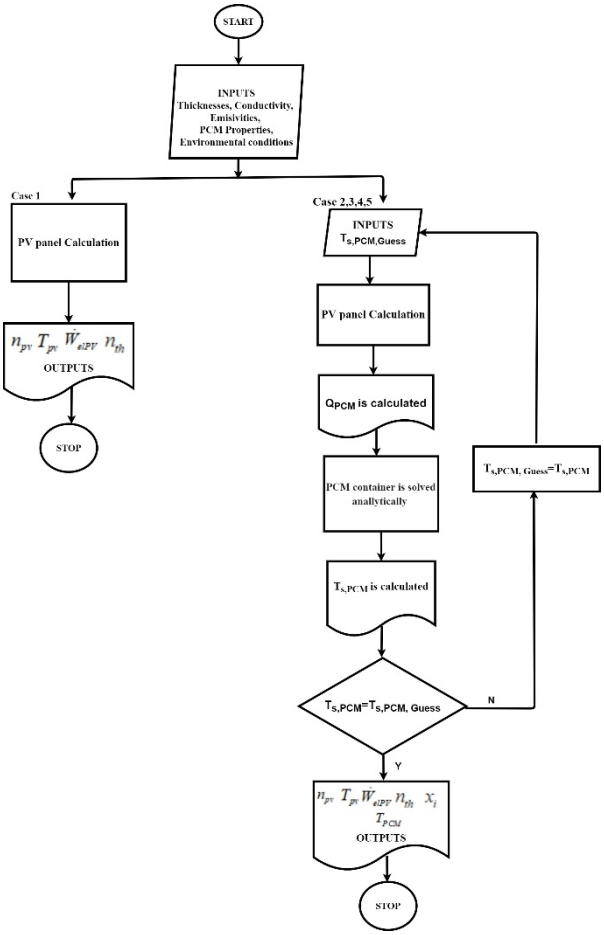

Fig. 4. Calculation procedure of the created models

3. Results and Discussions

After the model definition and solution procedure, in this section system outputs were examined under real environment conditions. However, first of all, the results obtained from the theoretical model were compared with the literature study in Section 3.1.

3.1. Verification of the 1-D theoretical model

The theoretical model used in this study was confirmed by the experimental and theoretical study made by Abdulmunem et al. [1] in the literature. The time-dependent variation of the PV panel temperature was used for verification. For verification, the PV panel area was taken as 0.0182 m2 and the irradiation was taken as 1000 W/m2. Fig. 5 shows the time-dependent PV panel temperatures for conventional PV panels and PV-PCM integration. When the current model was compared with the literature study, it was seen that the maximum temperature difference was 2.5ºC for the conventional PV panel, and 5 ºC for the PV-PCM integration. These temperature differences show that the current model was usable.

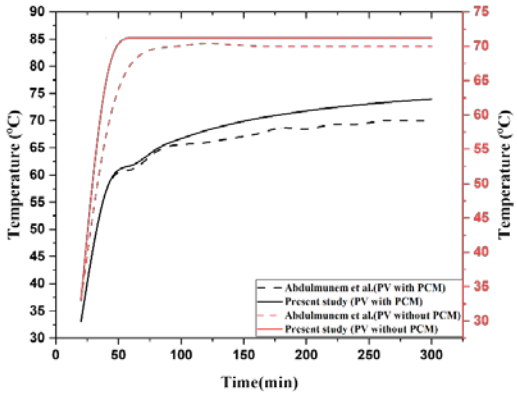

Fig. 5. Comparison of current model and literature study in terms of PV panel temperature

3.2. Climate conditions

In this study, real environmental conditions were preferred for investigations. Meteorological data were taken from Antalya, a province in Turkey [25]. As can be seen in Fig 5, Antalya province is located in the south of Turkey and is one of the provinces with the highest amount of irradiation and sunbathing time.

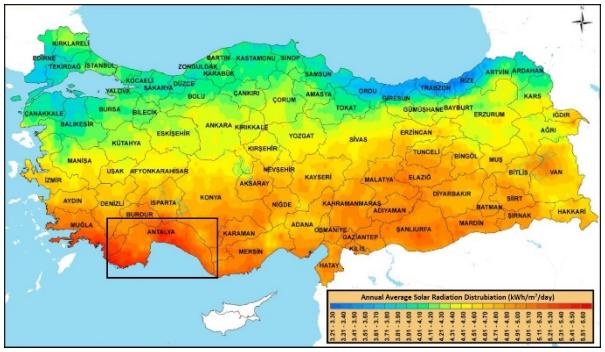

Fig. 6. Antalya province location in Turkey and annual avarage solar radiation distribution of TURKEY

Fig. 7 shows the irradiation, sunbathing time, ambient air temperature, and wind speeds depending on the month. While the most radiation was observed in March, the most sunbathing time was observed in July. In addition, the highest air temperature was observed in July, while the highest wind speed was observed in January. As it can be seen from the graphs, since the parameters show similarity seasonally, the evaluations in this study were made based on seasonal average meteorological data.

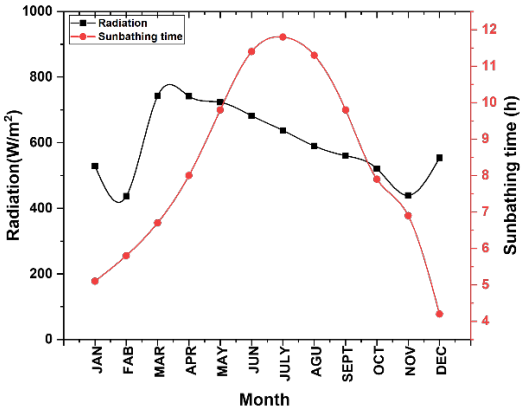

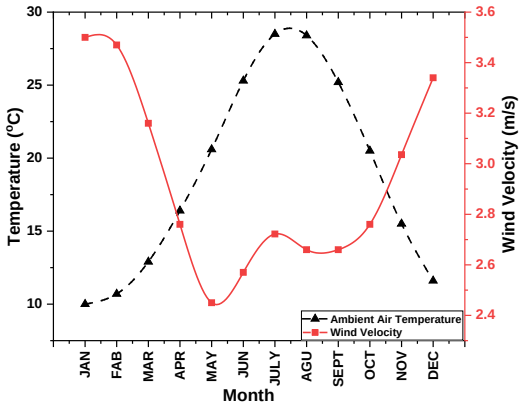

Fig.7. Meteorological data depending on the months.

Seasonal average meteorological data are given in Table 3. Accordingly, the months of December, January, and February represent the Winter season, March, April, and May represent the Spring season, June, July, and August represent the Summer season, and September, October, and November represent the Autumn season. System outputs according to these four seasons were shared in Section 3.3, and advantages and disadvantages were examined.

Table 3. Average seasonal meteorological data [25]

	Spring	Summer	Autumn	Winter
Avarage Ambient Temperature (°C)	16.6	27.4	20.4	10.07
Wind Velocity (m/s)	2.77	2.63	2.8	3.43
Radiation (W/m2)	506.75	636.5	735.9	506.58
Sunabathing time (hours)	8.16	11.5	8.2	5.03

3.3. Examining system outputs

In this section, seasonal PV panel temperature (T_{pv}), PCM melting rate ($\frac{x_i}{L_{cont}}$), electrical power generated ($\dot{W}_{el}$), energy absorbed by PCM ($\dot{Q}_{abs}$), PV (n_{pv}) and thermal efficiencies (n_{th}) were examined. The results shown below were analyzed based on sunbathing time for $T_{pv}$and PCM melting rate, while total seasonal for $\dot{Q}_{abs}$, $\dot{W}_{el}$, n_{pv} and n_{th}.

Initially, the results for the Spring season were shared in Fig. 8. Fig. 8a shows the PV panel temperatures during the sunbathing time. Accordingly, the temperature increased linearly during the 6000 seconds and remained stable for all cases. While there were small temperature differences between cases for stable conditions, the lowest PV panel temperatures were obtained for Case 1 and Case 3 approximately at 27°C at the end of sunbathing time. Fig. 8b shows the PCM melting rate during the sunbathing time. the PCM in the container did not melt completely in all 5 cases. the highest melting was obtained for Case 5 as 0.3 and the lowest melting was obtained for Case 3 as 0.06 , Fig.8c shows the seasonal average n_{pv},n_{th}, $\dot{Q}_{abs}$and $\dot{W}_{el}$. Maximum 1% differences were observed between n_{pv}'s (19-20%), Because of low differences between the PV panel temperatures (Fig. 7a) for each case. The maximum electricity generation was obtained for Case 3 and Case 1 as approximately 56000 W. $\dot{Q}_{abs}$ and n_{th} values was shown parallel behavior and reach the maximum value for Case 2 ($n_{th} = 10\%$,$\dot{Q}_{abs} = 4800W$) and Case 5 ($n_{th} = 11\%$,$\dot{Q}_{abs} = 5500W$).

The results for the spring showed that $T_{pv}$and n_{pv} did not change significantly in different conditions.

However, n_{th} and $\dot{Q}_{abs}$ varied considerably and it was found that a significant amount of heat energy could be stored in the PCM.

a)

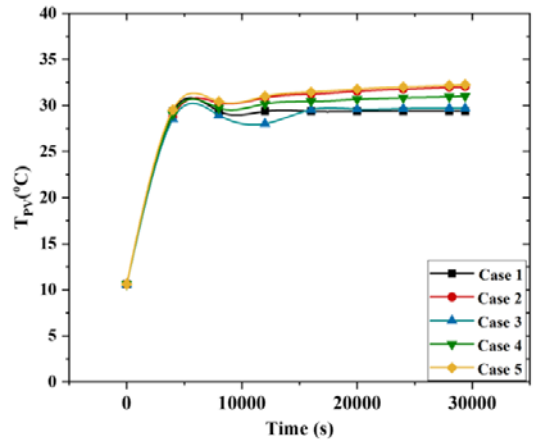

b)

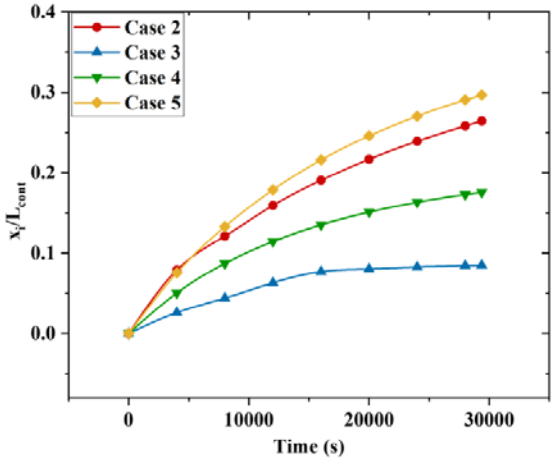

c)

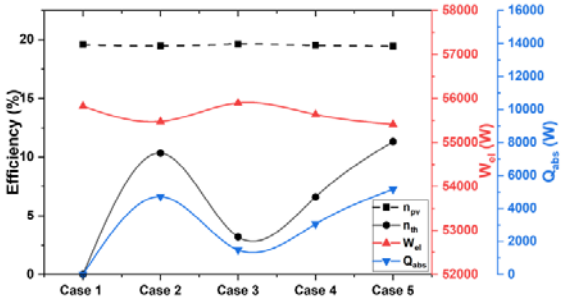

Fig. 8. a) T_{pv} b) $\frac{x_i}{L_{cont}}$ c) $\dot{W}_{el}$,n_{pv},n_{th},$\dot{Q}_{abs}$values for the Spring season

In Fig. 9, the system outputs for the summer season are shown. As seen in Fig. 9a, the maximum PV panel temperature was obtained for Case 2 at 47.5 °C and the minimum PV panel temperature was obtained for Case 3 at 40 °C. During the sunbathing time, the PV panel temperatures of Case 3 and 4 remained below Case 1 (conventional PV panel) and, in Case 1 and 2, after 15000 seconds, the PV panel temperature increased above Case 1. At the end of the sunbathing time, all of the PCM in the container was molten in Case 2 as seen in Fig. 9b. Also the lowest melting was seen for Case 3 as approximately 0.4. Although the n_{pv} values for each case are close to each other, Due to the low PV panel temperature, the highest n_{pv} was obtained as 19% for Case 3. Similarly, depending on the increase in n_{pv}, the $\dot{W}_{el}$ was obtained approximately 92200 W for the lowest Case 1 and 94500 W for the highest Case 3 as seen in Fig 9c. Due to the high melting rate, the highest $\dot{Q}_{abs}$ and n_{th} were determined as 11000 W and 20% for Case 2, respectively.

The results showed that the maximum system outputs

occurred for the Summer season. Therefore, it was shown that PV/PCM integrations are beneficial in summer conditions.

a)

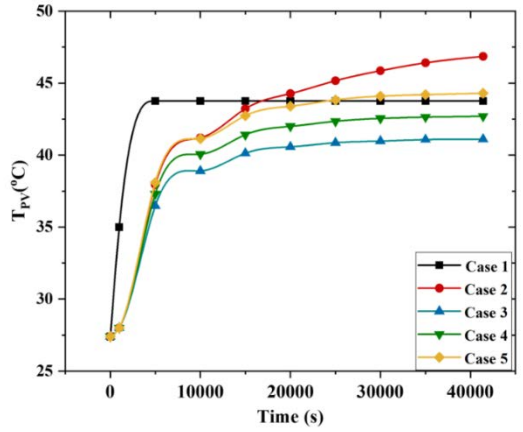

b)

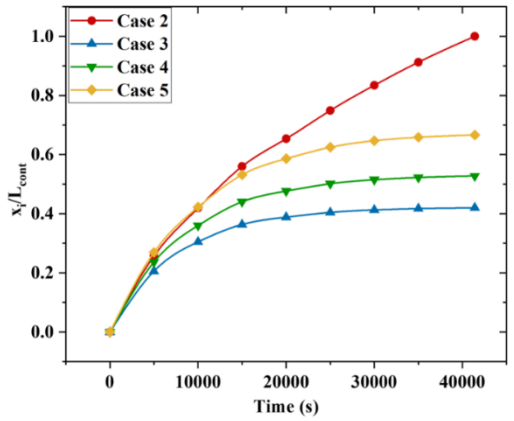

c)

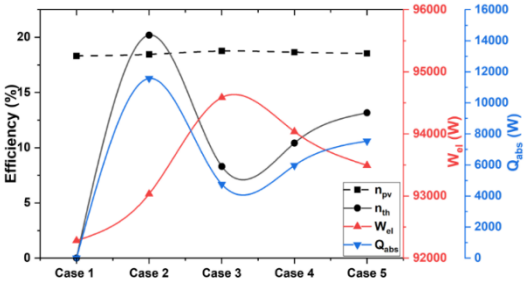

Fig. 9. a) T_{pv} b) $\frac{x_i}{L_{cont}}$ c) $\dot{W}_{el}$,n_{pv},n_{th},$\dot{Q}_{abs}$values for the Summer season

In the autumn season, similar to the summer season, the highest PV temperatures were obtained in Case 1 until the reached equilibrium (Fig 10a). After the temperatures reach equilibrium, only Case 3 temperature was lower than Case 1. At the end of the sunbathing time, the maximum PV panel temperature was obtained at approximately 43 ºC for Case 2 and, the minimum PV panel temperature was obtained at approximately 38 ºC for Case 3. Considering the melting rates, the maximum melting rate was obtained as approximately 0.6 for Case 2 and Case 5. Also the minimum melting rate was obtained for Case 3 as 0.3. As can be seen in Fig 10c, due to the closeness of the PV panel temperatures, there were no large differences between the n_{pv} for each case, and the highest n_{pv} value was obtained for Case 3 as 18.75%. Similarly, $\dot{W}_{el}$ values were very close to each other for each case and range from 78700 W (Case 3) to 78000 W (Case 5). Finally, The highest $\dot{Q}_{abs}$ and n_{th} values were obtained for Case 2 as 11000 W and 16%, respectively. The lowest values were obtained for Case 3 as 7000 W and 8.5%, respectively.

Since autumn meteorological data were close to summer meteorological data, the use of PV/PCM integration was appropriate for autumn.

a)

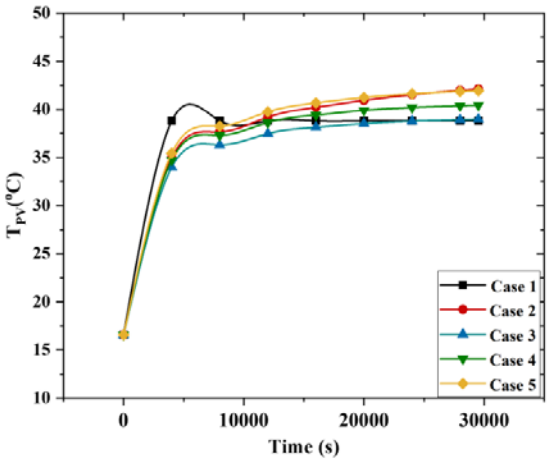

b)

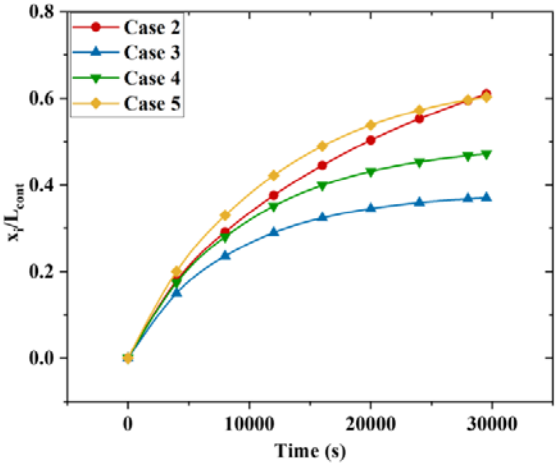

c)

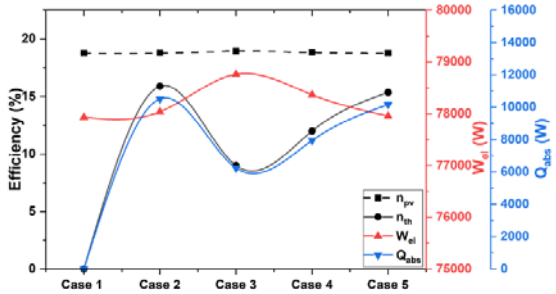

Fig. 10. a) T_{pv} b) $\frac{x_i}{L_{cont}}$ c) $\dot{W}_{el}$,n_{pv},n_{th},$\dot{Q}_{abs}$values for the Autumn season

The results are quite different for the Winter season as can be seen in Fig.11. In winter, melting was not occurred in the PCM container due to low irradiation, ambient temperatures, and high wind speed. Therefore, all PV-PCM integrations reached a higher PV panel temperature than conventional PV panels. The maximum PV panel temperature was obtained at 33 ºC for Case 5 and the minimum PV panel temperature was obtained at 21.5 ºC for Case 1. The electrical efficiency and electricity production were similarly maximum in the conventional PV panel as 35750 W and 20.5%. Therefore, It has been seen that the PV-PCM integration was not suitable for the Winter season.

a)

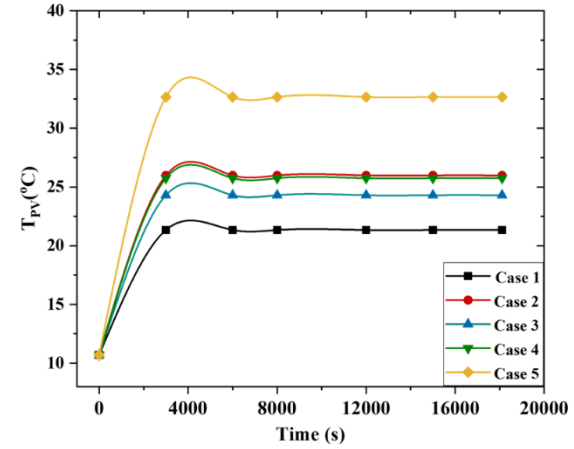

b)

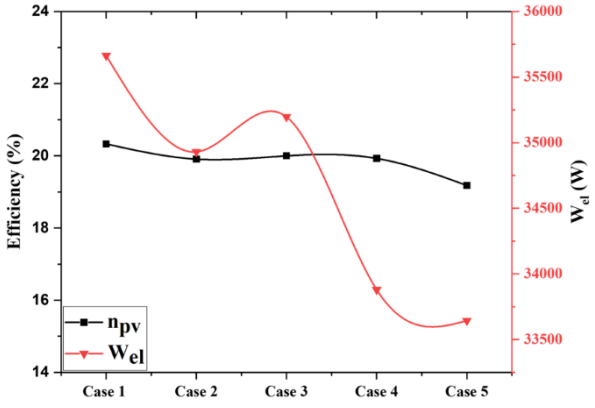

Fig. 11. a) T_{pv} b) $\dot{W}_{el}$,n_{pv} values for the Autumn season

As mentioned above, all of the PCM in the container melted in Case 2 during the summer season. Therefore, the PCM temperature during melting for Case 2 is seen in Fig. 12. The results showed that the maximum temperature (x=0) increased from 42 ºC to 48 ºC depending on time In addition, a linear temperature drop was seen in the liquid phase which the melting takes place, at x-direction, but there were no significant temperature differences were seen in the solid phase. Therefore, it has been determined that the heat conduction in the solid phase was negligible.

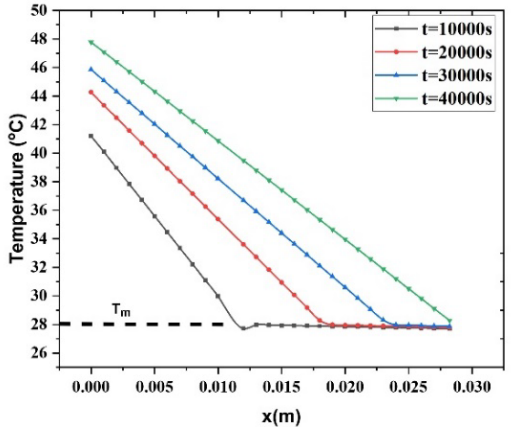

Fig.12. Time dependent temperature distribution of PCM

Until this part, the seasonal performance of the 1 m2 area PV panel has been examined. However, in practice, more PV panels are used for high electrical power generation. Therefore, Fig. 12 shows the annual PV panel performance for a 1000 m2 panel area. The results showed that Case 3 and Case 4 produced 1200 kW and 230 kW more electricity than Case 1 respectively, and Case 2 and Case 5 produced 220 kW and 970 kW less electricity respectively than a Case 1. Considering the $\dot{Q}_{abs}$ values, the highest $\dot{Q}_{abs}$ value was obtained in Case 2 as 26990 kW, while in Case 3,4, and 5 less energy was stored in PCM than in Case 2 as 16766, 10020, and 4120 kW respectively.

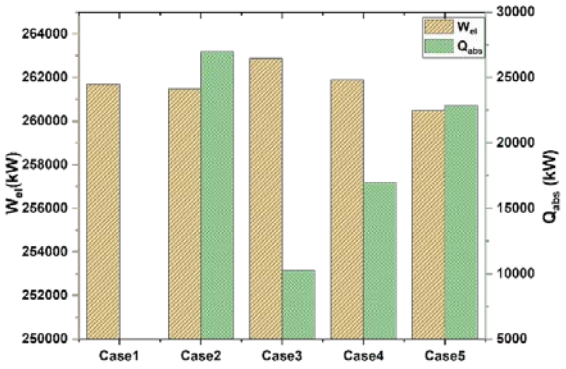

Fig.13. Annual $\dot{W}_{el}$ and $\dot{Q}_{abs}$values for each case and 1000 m2 panel area

4. Conclusion

In this study, PCM was used in different configurations to cool the PV panel and compared with the conventional PV panel. The study was carried out for 5 different cases. In the first case conventional PV panel, in the second case PV-PCM integration, and in the third, fourth, and fifth cases, PV-PCM integration at base temperatures of 10, 15, and 20 oC were investigated. The investigations were carried out using real meteorological data for Antalya, a province in Turkey. In order to, evaluate the PV panel cooling performance and melting rate of the PCM in the long term, PV panel temperatures were calculated based on the daily sunshine duration in the study. In addition, seasonal average $\dot{W}_{el}$, $\dot{Q}_{abs}$, n_{pv},n_{th},temperature distribution of PCM during melting were calculated. A 1-D mathematical model was used for the calculations and confirmed by the study in the literature.

The following results were obtained within the scope of the study.

- It has been observed that the PV panel temperature (Case 1) was highly affected by seasonal environmental conditions. The maximum PV panel temperature for the summer season was obtained at 45 ºC. For the winter season, this value decreased to 22 ºC. Although it is thought that placing the PCM on the PV panel base reduces the temperature of the PV cells, it was determined that the temperature of the PV cells was negatively affected depending on the meteorological data and the sunbathing duration for some cases.
- When T_{pv}, $\dot{W}_{el}$ and n_{pv} values were examined in the Spring season, only Case 3 gave better results than Case 1. Therefore, it was revealed that the bottom of the PCM container should be kept at a low temperature for the autumn season.
- All cases gave positive results from Case 1 for T_{pv}, $\dot{W}_{el}$, and n_{pv} values in Summer. Therefore, it was determined that the use of PCM was very necessary for high air temperature, high radiation values, low wind speed, and high sun exposure times.
- Case 3 and Case 4 gave better results than Case 1 for T_{pv}, $\dot{W}_{el}$, and n_{pv} values in the Autumn season, but Case 2 and Case 5 gave very close results to Case 1. Therefore, it was found that cooling the bottom of the PCM container during the Autumn season improves the results.
- It has been observed that PV-PCM integrations for the winter season gave worse results compared to Case 1.
- When $\dot{Q}_{abs}$ and n_{th} values were examined, they were quite high especially for Summer and Autumn seasons. In this case, it was seen that the stored energy could be benefited at the end of the sunbathing period.

With the help of the results obtained in this study and the mathematical model, it is thought that researchers can easily design PV-PCM depending on changing environmental conditions.

Declaration of conflicting interests

The authors declare no competing interests.

Funding

The author received no financial support for the research and/or authorship of this article.

References

[1] Abdulmunem, A. R., Samin, P. M., Rahman, H. A., Hussien, H. A., Mazali, I. I., & Ghazali, H. "Numerical and experimental analysis of the tilt angle's effects on the characteristics of the melting process of PCM-based as PV cell's backside heat sink." *Renewable Energy*, 173, 520-530,2021.

[2] Abdulmunem, A.R. "Passive cooling by utilizing the combined PCM/aluminum foam matrix to improve solar panels performance: indoor investigation," *Iraqi J. Mech. Mater. Eng* 17(4): 712-723,2017.

[3] Huang, M. J., Eames, P. C., & Norton, B. "Thermal regulation of building-integrated photovoltaics using phase change materials." *International Journal of heat and mass transfer*, 47(12-13), 2715-2733,2004

[4] Bilgen, E. "Passive solar massive wall systems with fins attached on the heated wall and without glazing."*J. Sol. Energy Eng.*, *122*(1), 30-34, 2000.

[5] Goossens, D., & Van Kerschaever, E. "Aeolian dust deposition on photovoltaic solar cells: the effects of wind velocity and airborne dust concentration on cell performance." *Solar energy*, *66*(4), 277-289,1999.

[6] Emam, M., & Ahmed, M. "Cooling concentrator photovoltaic systems using various configurations of phase-change material heat sinks." *Energy conversion and management*, *158*, 298-314,2018.

[7] Ling, Z., Zhang, Z., Shi, G., Fang, X., Wang, L., Gao, X., ... & Liu, X. "Review on thermal management systems using phase change materials for electronic components, Li-ion batteries and photovoltaic modules." *Renewable and Sustainable Energy Reviews*, *31*, 427-438,2014.

[8] Ma, T., Li, Z., & Zhao, J. "Photovoltaic panel integrated with phase change materials (PV-PCM): technology overview and materials selection." *Renewable and Sustainable Energy Reviews*, *116*, 109406,2019.

[9] Armstrong, S., & Hurley, W. G. "A thermal model for photovoltaic panels under varying atmospheric conditions." *Applied thermal engineering*, *30*(11-12), 1488-1495,2010.

[10] Smith, C. J., Forster, P. M., & Crook, R. "Global analysis of photovoltaic energy output enhanced by phase change material cooling." *Applied energy*, *126*, 21-28,2014.

[11] Stritih, U. "Increasing the efficiency of PV panel with the use of PCM." *Renewable Energy*, *97*, 671-679, 2016.

[12] Khanna, S., Reddy, K. S., & Mallick, T. K. "Performance analysis of tilted photovoltaic system integrated with phase change material under varying operating conditions." *Energy*, *133*, 887-899,2017.

[13] Savvakis, N., & Tsoutsos, T. "Theoretical design and experimental evaluation of a PV+ PCM system in the mediterranean climate." *Energy*, *220*, 119690, 2021.

[14] Ahmadi, R., Monadinia, F., & Maleki, M. " Passive/active photovoltaic-thermal (PVT) system implementing infiltrated phase change material (PCM) in PS-CNT foam." *Solar Energy Materials and Solar Cells*, *222*, 110942,2021.

[15] Duan, J. "The PCM-porous system used to cool the inclined PV panel."*Renewable Energy*, *180*, 1315-1332,2021.

[16] Ashouri, M., & Hakkaki-Fard, A. "Improving the performance of the finned absorber inclined rooftop solar chimney combined with composite PCM and PV module." *Solar Energy*, *228*, 562-574,2021.

[17] Khodadadi, M., & Sheikholeslami, M. " Numerical simulation on the efficiency of PVT system integrated with PCM under the influence of using fins." *Solar Energy Materials and Solar Cells*, *233*, 111402,2021.

[18] Khanna, S., Reddy, K. S., & Mallick, T. K. " Optimization of finned solar photovoltaic phase change material (finned pv pcm) system." *International Journal of Thermal Sciences*, *130*, 313-322,2018.

[19] Kumar, K. S., Kumar, H. A., Gowtham, P., Kumar, S. H. S., & Sudhan, R. H. "Experimental analysis and increasing the energy efficiency of PV cell with nano-PCM (calcium carbonate, silicon carbide, copper)."*Materials Today: Proceedings*, *37*, 1221-1225,2021.

[20] Stalin, P. M. J., Prasad, K. S., Kumar, K. P., Hemadri, G., Rajesh, M., & Kumar, K. P. " Performance improvement of solar PV through the thermal management using a nano-PCM."*Materials Today: Proceedings*, *50*, 1553-1558,2022.

[21] Kurşun, B., & Ökten, K. "Thermodynamic analysis of a Rankine cycle coupled with a concentrated photovoltaic thermal system for hydrogen production by a proton exchange membrane electrolyzer plant."*International Journal of Hydrogen Energy*, *44*(41), 22863-22875,2019.

[22] Cengel, Y.A. and Ghajar, A.J.J.A.p.a., 2007, *Heat and mass transfer*,2007

[23] Chow, T. T. "Performance analysis of photovoltaic-thermal collector by explicit dynamic model."*Solar Energy*, *75*(2), 143-152,2003.

[24] Jiji, L. M., & Gaye, S. "Analysis of solidification and melting of PCM with energy generation." *Applied Thermal Engineering*, *26*(5-6), 568-575,2006.

[25] Ökten, K. "Investigationof PV Panel Integrated PCM-Nanoparticle Mixture Using 1-D Mathematical Model" *Gazi University Journal of Science Part C: Design and Technology*, *10*(3), 532-546,2022.